Frontiers in Bioscience Landmark

Front. Biosci. (Landmark Ed) **2023**; 28(12): 324
https://doi.org/10.31083/j.fbl2812324

Original Research

EGCG Restores Keratinocyte Autophagy to Promote Diabetic Wound Healing through the AMPK/ULK1 Pathway

Chao Tian[1,†], Yuchao Feng[1,†], Tianhua Chen[1], Zuyang Zhang[1], Xiaojie He[2], Liangdong Jiang[1,*], Mingjiang Liu[1,*]

[1]Department of Orthopaedics, The Affiliated Changsha Central Hospital, Hengyang Medical School, University of South China, 410004 Changsha, Hunan, China
[2]Institute of Pediatrics, Laboratory of Pediatric Nephrology, Central South University, 410011 Changsha, Hunan, China
*Correspondence: 2018050831@usc.edu.cn (Liangdong Jiang); 15228449@qq.com (Mingjiang Liu)
[†]These authors contributed equally.
Academic Editor: Luigi De Masi
Submitted: 18 April 2023 Revised: 3 July 2023 Accepted: 17 July 2023 Published: 1 December 2023

Abstract

Background: Delayed wound healing, a common problem in patients with diabetes mellitus (DM), is associated with impaired keratinocyte autophagy. Epigallocatechin gallate (EGCG), a catechin, has been proven to promote diabetic wound healing. This study aims to explore the therapeutic mechanism of EGCG on diabetic wound healing. **Methods**: High glucose (HG)-induced keratinocytes and streptozotocin (STZ)-induced DM rats were prepared and intervened with EGCG to examine its therapeutic effects in *in vivo* and *in vitro* settings. The AMPK inhibitor, Compound C, was utilized to determine whether EGCG exerted its therapeutic effects through the AMPK/ULK1 pathway. **Results**: *In vitro*, EGCG improved HG-induced autophagy impairment in keratinocytes by increasing LC3II/LC3I, Becline1, and ATG5 levels and decreasing p62 level. Mechanically, EGCG activated the AMPK/ULK1 pathway, thereby promoting keratinocyte autophagy through the phosphorylation of AMPK and ULK1. Notably, EGCG promoted the proliferation, migration, synthesis and release of C-C motif chemokine ligand 2 (CCL2) in HG-treated keratinocytes. Furthermore, EGCG indirectly promoted the activation of fibroblasts, as evidenced by increased alpha-smooth muscle actin (α-SMA) and Collagen I levels. *In vivo*, EGCG promoted wound healing in DM rats, primarily by reducing inflammatory infiltration and increasing granulation tissue to promote wound epithelialization. Besides, EGCG promoted ATG5, KRT10, KRT14, TGF-β1, Collagen I, and α-SMA expressions in the neonatal epithelial tissues of DM rats. However, the use of Compound C reversed the effects of EGCG. **Conclusions**: These findings indicated that EGCG restored keratinocyte autophagy to promote diabetic wound healing through the AMPK/ULK1 pathway.

Keywords: diabetic cutaneous ulcers (DCU); epigallocatechin gallate (EGCG); AMPK/ULK1 pathway; keratinocytes; autophagy

1. Introduction

Diabetic cutaneous ulcers (DCU) are one of the complications of diabetes mellitus (DM) [1]. Glucose metabolism disorder, neuropathy, blood circulation disorder, and local infection are considered important factors causing the onset of DCU [2]. Clinically, DCU treatment includes debridement and dressing changes, infrared radiation, injection or oral administration of hypoglycemic drugs, and even amputation surgery in severe cases [3]. The long duration of treatment, high recurrence rate, and disability rate of DCU bring great physical and mental pain and economic burden to patients and families [4]. Promoting early wound healing in DCU and reducing its disability rate and treatment cost remain challenging. Therefore, it is urgent to further explore the pathogenesis of DCU, identify potential therapeutic targets, and develop new therapeutic methods.

Epigallocatechin gallate (EGCG), a main active component in green tea, possesses several biological activities such as anti-inflammatory [5], antioxidant [6], hypoglycemic [7], antibacterial [8], and anticancer [9]. EGCG has displayed remarkable potential in wound healing, as shown through *in vitro* and *in vivo* studies [10]. In a study of skin inflammation, EGCG can reduce the basal release and upregulation of vascular endothelial growth factor (VEGF) and interleukin-8 (IL-8) in normal human keratinocytes stimulated by tumor necrosis factor-α (TNF-α) [11]. Besides, both zonal priming and direct application of EGCG have been shown to promote cutaneous scarring therapy by reducing mast cells, skin thickness, angiogenesis, and so on [12]. In DM mice, EGCG has been demonstrated to improve wound healing by reducing macrophage-mediated inflammation through the Notch signaling pathway [13]. Therefore, EGCG may be a feasible alternative to current DCU therapies. Wound healing can be subdivided into four stages, including hemostasis, inflammation, proliferation and tissue remodeling [10]. The mechanism of skin wound healing is very complex, involving various types of cells (such as immune cells, fibroblasts, and keratinocytes), various biochemical processes, and the synergistic effects of various factors (such as cytokines, chemokines, growth factors, and enzymes). Although EGCG can promote skin wound healing, its specific mechanism of action still needs

further clarification. Further research can help discover new regulatory pathways and targets, providing a theoretical basis for developing new drugs for wound healing in DM patients.

Skin wound healing is a complex process that requires collaboration between cells located in different layers of the skin [14]. During the proliferation stage of wound healing, cells from the epidermis and dermis proliferate and migrate to the wound bed to close the wound [15]. Keratinocytes in the epidermis are essential in wound healing. In DCU, keratinocytes exhibit reduced proliferation and impaired migration [16]. Autophagy, an important cellular process, plays a key role in maintaining cell homeostasis. Autophagy disorder contributes to the occurrence of skin diseases and delayed wound healing [17]. High glucose (HG) hinders keratinocyte autophagy by reducing autophagy-related protein 5 (ATG5), p62, and microtubule-associated protein 1 light chain 3 (LC3II) expressions and inhibiting keratinocyte migration, thereby delaying DCU wound healing [18]. Fibroblasts have been identified as key players in skin repair, responsible for the regeneration of granulation tissue as well as re-epithelialization [19,20]. During wound healing, keratinocytes induce C-C motif chemokine 2 (CCL2) expression through autophagy, and the abundance of CCL2 is required to promote keratinocyte proliferation and migration and fibroblast activation [21]. Thus, the restoration of keratinocyte autophagy may be a promising method to promote wound healing in DCU.

AMP-activated protein kinase (AMPK) is an energy sensor capable of regulating a variety of metabolic and physiological processes [22]. However, AMPK activity is impaired in DM and its complications [23]. A previous study revealed that drugs that activate and regulate AMPK can enhance glucose uptake by cells and inhibit its intracellular production, offering a potential therapeutic effect on DM and its complications [24]. Additionally, the AMPK/Unc-51-like kinase-1 (ULK1) pathway is an important pathway involved in regulating autophagy. Inhibition of this pathway can reduce autophagosome production and downregulate LC3 and Beclin1 expressions [25,26]. AMPK regulates autophagy via the direct phosphorylation of ULK1 [27]. These findings suggest that enhancing AMPK/ULK1-mediated autophagy may help to reduce the risk of DM and its complications [28,29]. The study has found that EGCG can induce autophagy by enhancing AMPK activity, and ULK1 is crucial for EGCG-induced autophagy [30]. However, the role of EGCG in DCU by regulating AMPK/ULK1-mediated autophagy has not been reported.

Therefore, HG-induced cell models and streptozotocin (STZ)-induced DM rat models were constructed and intervened with EGCG to determine whether EGCG could restore keratinocyte autophagy, promote the activation of keratinocytes and fibroblasts, as well as accelerate wound healing in DCU by activating the AMPK/ULK1 pathway.

2. Materials and Methods

2.1 Cell Culture

Keratinocytes (HaCaT, AW-CNH203, Abiowell, Changsha, China) and fibroblasts (HFF-1, AW-CCH222, Abiowell, Changsha, China) were cultured in Dulbecco's modified Eagle's medium (DMEM, D5796, Sigma, Saint. Louis, MO, USA) and RPMI-1640 medium (2144322, Biological Industries, Kibbutz Beit-Haemek, Israel). These medium were supplemented with 10% of fetal bovine serum (FBS, 10099141, Gibco, Carlsbad, CA, USA) and 1% of Penicillin/Streptomycin (AWI0070a, Abiowell, Changsha, China). They were placed in an incubator (DH-160I, SANTN, Shanghai, China) containing 5% CO_2 at 37 °C. In addition, cell slides were prepared by respective inoculation of appropriate densities of HaCaT and HFF-1 cells in culture dishes for Immunofluorescence (IF) staining and 5-Ethynyl-2′-deoxyuridine (EdU) staining analysis. The purchased Cell lines have been authenticated by short tandem repeat (STR) profiling. All the cells used in the experiment were tested and confirmed to be free of mycoplasma contamination.

2.2 Cell Grouping and Treatment

For HaCaT cells, grouping 1 included 0 µM EGCG, 6.25 µM EGCG, 12.5 µM EGCG, 25 µM EGCG, 50 µM EGCG, and 100 µM EGCG. Grouping 2 included Control, HG, HG + 6.25 µM EGCG, HG + 12.5 µM EGCG, HG + 25 µM EGCG, and HG + 50 µM EGCG. The HaCaT cells in the Control group were cultured normally. The HaCaT cells in the other groups were treated with HG (50 mM glucose) for 24 h and EGCG (2503504, Shanghai Yuanye Bio-Technology Co., Ltd., Shanghai, China) at different concentrations for 24 h [31]. Grouping 3 included Control, HG, HG + EGCG, and HG + EGCG + Compound C. Except for the Control group, HaCaT cells in other groups were treated with HG for 24 h. HaCaT cells in the HG + EGCG group were treated with 50 µM EGCG for 24 h after HG induction. HaCaT cells in the HG + EGCG + Compound C group were treated with 50 µM Compound C (D426448, Aladdin, Shanghai, China) and 50 µM EGCG for 24 h after HG induction [32]. The information about the processing of different groups was shown in Table 1. To induce the synthesis and release of CCL2, cells in each group were treated with 100 ng/mL TNF-α (MAB610-SP, R&D Systems, Minneapolis, MN, USA) for 24 h [21]. For HFF-1 cells, groups included Control, HG, HG + EGCG, and HG + EGCG + Compound C. TNF in the supernatant of HaCaT cells in grouping 3 was neutralized with 2 µg/mL anti-TNF-α antibody (AF-410-SP, R&D Systems, Minneapolis, MN, USA), and then the supernatant was added to HFF-1 cells for 48 h, respectively (the supernatant content was 20%).

2.3 Animal Modeling and Intervention

Male adult Sprague-Dawley rats (SPF, 7–8 weeks, 180–200 g) were bought from Hunan SJA Laboratory An-

Table 1. Processing of different groups in cell experiments.

	Group name	HG induction	EGCG	Compound C
Grouping 1	0 μM EGCG	-	-	-
	6.25 μM EGCG	-	6.25 μM	-
	12.5 μM EGCG	-	12.5 μM	-
	25 μM EGCG	-	25 μM	-
	50 μM EGCG	-	50 μM	-
	100 μM EGCG	-	100 μM	-
Grouping 2	Control	-	-	-
	HG	+	-	-
	HG + 6.25 μM EGCG	+	6.25 μM	-
	HG + 12.5 μM EGCG	+	12.5 μM	-
	HG + 25 μM EGCG	+	25 μM	-
	HG + 50 μM EGCG	+	50 μM	-
Grouping 3	Control	-	-	-
	HG	+	-	-
	HG + EGCG	+	50 μM	-
	HG + EGCG + Compound C	+	50 μM	50 μM

EGCG, Epigallocatechin gallate; HG, High glucose.

Table 2. Processing of different groups in animal experiments.

	Group name	STZ induction	EGCG	Compound C
Grouping 1	Normal	-	-	-
	DM	80 mg/kg	-	-
	DM + EGCG	80 mg/kg	1 mg/mL	-
	DM + EGCG + Compound C	80 mg/kg	1 mg/mL	1 mg/kg

Notes: EGCG, Epigallocatechin gallate; DM, diabetes mellitus; STZ, streptozotocin.

imal Co., Ltd. (Changsha, China). After adaptive feeding, rats were randomly divided into Normal, DM, DM + EGCG, and DM + EGCG + Compound C groups with 10 rats in each group. The DM rat model was established according to a previously described method [33]. Rats were intraperitoneally injected with STZ (80 mg/kg) (AWH0492a, Abiowell, Changsha, China) dissolved in citrate buffer solution (0.1 M, pH 4.5) to induce type I DM [34], with the same dose of citrate buffer solution being the control in the Normal group. Follow-up experiments were performed when the blood glucose level reached 16.7 mM. After the rats were anesthetized with intraperitoneal injection of 1% pentobarbital (30 mg/kg), a 15 mm diameter wound was created on the back using the full-thickness skin defect method. Rats in Normal and DM groups were treated daily with 1% carboxymethyl cellulose (C501052, Aladdin, Shanghai, China). Rats in the DM + EGCG group were treated with 1 mg/mL EGCG daily [35]. Rats in the DM + EGCG + Compound C group were given 1 mg/kg Compound C near the wound at 30 min before EGCG intervention [36]. The information about the processing of different groups was shown in Table 2. On days 0, 3, 7, and 14, the wound area was measured and photographed, and the wound healing rate was calculated according to the methods described in the literature [35]. On day 14, rats were sacrificed by cervical dislocation, and neonatal epithelial tissues were taken for follow-up analysis.

2.4 Cell Counting Kit-8 (CCK-8) Assay

HaCaT cells in the logarithmic growth phase were digested with trypsin (AWC0232, Abiowell, Changsha, China) to prepare a cell suspension. Cells were inoculated into 96-well plates at a density of 1×10^4 cells/well. After adherent growth, cells were treated with EGCG for 24 h. After the removal of the EGCG-containing medium, 100 μL of medium containing 10% CCK-8 reagent (NU679, DOJINDO, Kumamoto, Japan) was added. After being incubated for 4 h, the cells were analyzed with a multifunctional microplate reader (MB-530, HEALES, Shenzhen, China) to obtain the optical density (OD) at 450 nm.

2.5 Western Blot

Total proteins were extracted from HaCaT cells and neonatal epithelial tissues using RIPA lysate (AWB0136, Abiowell, Changsha, China). The proteins were separated by sodium dodecyl sulfate-polyacrylamide gel electrophoresis (SDS-PAGE) and transferred to nitrocellulose (NC) membranes. NC membranes were blocked with 5% skimmed milk (AWB0004, Abiowell, Changsha, China) and incubated with the following primary an-

tibodies respectively, including p62 (1:10,000, 66184-1-Ig, Proteintech, Chicago, IL, USA), Beclin1 (1:2000, 11306-1-AP, Proteintech, Chicago, IL, USA), ATG5 (1:5000, ab108327, Abcam, Cambridge, UK), LC3 (2 µg/mL, ab48394, Abcam, Cambridge, UK), phosphorylated-AMPK (p-AMPK, 1:5000, ab92701, Abcam, Cambridge, UK), AMPK (1:5000, 10929-2-AP, Proteintech, Chicago, IL, USA), p-ULK1 (1:5000, 29006-1-AP, Proteintech, Chicago, IL, USA), ULK1 (1:20,000, ab133747, Abcam, Cambridge, UK), CCL2 (1:2000, 66272-1-Ig, Proteintech, Chicago, IL, USA), transforming growth factor-β1 (TGF-β1, 1:1000, ab235578, Abcam, Cambridge, UK), matrix metallopeptidase-9 (MMP-9, 1:1000, ab38898, Abcam, Cambridge, UK), Collagen I (1:1000, ab270993, Abcam, Cambridge, UK), and β-actin (1:5000, 66009-1-Ig, Proteintech, Chicago, IL, USA) Then, NC membranes were incubated with the following secondary antibodies respectively, including horseradish peroxidase (HRP)-goat anti-mouse IgG (1:5000, SA00001-1, Proteintech, Chicago, IL, USA) and HRP-goat anti-rabbit IgG (1:6000, SA00001-2, Proteintech, Chicago, IL, USA). NC membranes were incubated with Super ECL Plus detection reagent (AWB0005, Abiowell, Changsha, China) for chemiluminescence imaging. Quantity One 4.6.6 (Bio-Rad Inc., Hercules, CA, USA) was employed to obtain the gray values of protein bands, and the expression level of each protein was calculated with β-actin being an internal reference.

2.6 IF Staining

Cell slides were washed with phosphate-buffered saline (PBS), fixed with 4% paraformaldehyde, permeabilized with 0.3% Triton, and blocked with 5% bovine serum albumin (BSA). For tissue slices, antigen repair was performed after dewaxing to water. The tissue slices were washed with PBS, and sequentially placed in sodium borohydride solution, 75% ethanol solution, and Sudan black dye solution. After washing with PBS, the tissue slices were blocked with 5% BSA. The cell slides were incubated respectively with primary antibodies of LC3 (1:100, 14600-1-AP, Proteintech, Chicago, IL, USA), p62 (1:50, 18420-1-AP, Proteintech, Chicago, IL, USA), alpha-smooth muscle actin (α-SMA, 1:50, BM0002, Boster, Pleasanton, CA, USA), and Collagen I (1:100, 14695-1-AP, Proteintech, Chicago, IL, USA). The tissue slices were incubated respectively with primary antibodies of LC3, p62, ATG5 (1:50, 66744-1-Ig, Proteintech, Chicago, IL, USA), keratin 10 (KRT10, 1:50, 18343-1-AP, Proteintech, Chicago, IL, USA), and keratin 14 (KRT14, 1:50, 10143-1-AP, Proteintech, Chicago, IL, USA). The cell slides and tissue slices were incubated respectively with CoraLite488-conjugated Affinipure Goat Anti-Rabbit IgG (H + L) (1:200, SA00013-2, Proteintech, Chicago, IL, USA) or CoraLite594-conjugated Goat Anti-Mouse IgG (H + L) (1:200, SA00013-3, Proteintech, Chicago, IL, USA). Then, nuclei were stained with 4′,6-diamidino-2-phenylindole (DAPI) staining solution (AWI0331a, Abiowell, Changsha, China) and washed with PBS. The cell slides and tissue slices were sealed with buffered glycerin and the images were collected by a microscope (BA410T, Motic, Wetzlar, Germany).

2.7 EdU Staining

HaCaT cells (1×10^5) in the logarithmic growth stage were inoculated into 6-well plates, and then treated with corresponding drugs. According to the instructions of the EdU detection kit (C10310, RIBOBIO, Guangzhou, China), cells in each group were subjected to EdU labeling, immobilization, Apollo staining, and DNA staining, and images were collected by a fluorescence microscope.

2.8 Scratch Assay

The scratch assay was applied to detect the migration ability of HaCaT cells in each group. HaCaT cells from different groups were digested to make a cell suspension. The 5×10^5 cells were uniformly inoculated in 6-well plates. When the cells had filled the plates, lines were drawn and viewed under a microscope to record the initial scratch width. After 24 h and 48 h, the images were photographed with a microscope and scratch widths were measured using ImageJ 1.8.0 (National Institutes of Health, Bethesda, MD, USA).

2.9 Enzyme-Linked Immunosorbent Assay (ELISA)

The HaCaT cell cultures in different groups were centrifuged at 1000 g at 4 °C for 15 min, and the supernatant was used for detection. The content of CCL2 released to supernatant was assessed according to the instruction of the CCL2 ELISA kit (CSB-E04655h, CUSABIO, Wuhan, China).

2.10 Hematoxylin-Eosin (HE) Staining

The epithelial tissue slices were dewaxed in xylene and dehydrated with gradient ethanol (75–100%). They were stained with hematoxylin (AWI0001a, Abiowell, Changsha, China), and then returned to blue in PBS. Next, the slices were stained with eosin (AWI0029a, Abiowell, Changsha, China), and dehydrated with gradient alcohol (95–100%). The slices were cleared in xylene and then sealed with neutral gum (AWI0238a, Abiowell, Changsha, China) for observation with a microscope.

2.11 Immunohistochemistry (IHC) Staining

After being dewaxed to water, the epithelial tissue slices were immersed in citrate buffer (0.01 M, pH 6.0) (AWI0206a, Abiowell, Changsha, China), and boiled for antigen retrieval. Subsequently, the endogenous enzymes were inactivated with 1% periodic acid. The slices were incubated with the primary antibody of α-SMA (1:500, BM0002, Boster, Pleasanton, CA, USA) overnight followed by poly-HRP-anti-mouse-IgG. Next, diaminoben-

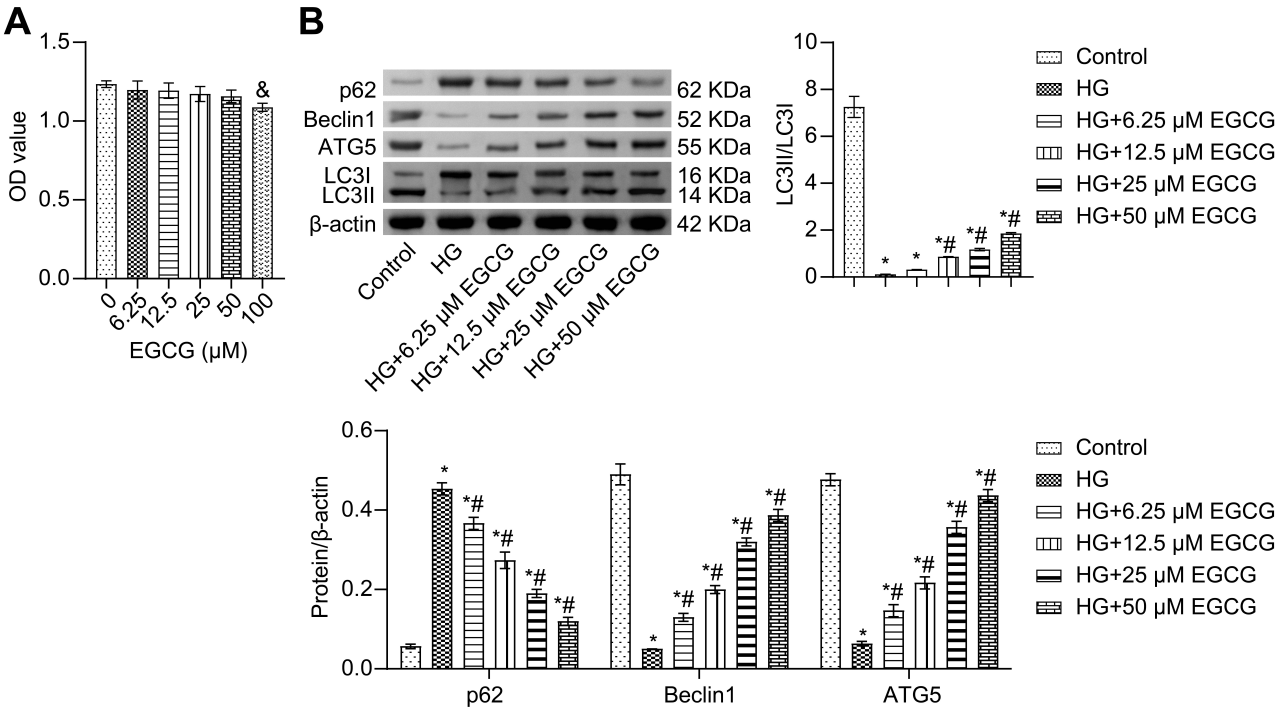

Fig. 1. EGCG induced autophagy in HG-treated keratinocytes. (A) The viability of keratinocytes treated with different concentrations of EGCG was evaluated by the CCK-8 assay. (B) The levels of p62, Beclin1, ATG5, LC3I, and LC3II in keratinocytes were analyzed by Western blot. &$p < 0.05$ *vs.* 0 μM EGCG, *$p < 0.05$ *vs.* Control, #$p < 0.05$ *vs.* HG.

zidine (DAB) was added to slices for catalytic color development. The slices were re-stained with hematoxylin, rinsed with distilled water, returned to blue in PBS, and dehydrated with gradient alcohol (60–100%). After being cleared in xylene and sealed with neutral gum, the slices were observed by a microscope.

2.12 Masson Staining

The epithelial tissue slices were dewaxed to water and stained with hematoxylin. They were washed with tap water and distilled water in turn. Next, the slices were soaked in PBS to make the nucleus return blue and stained with an acid fuchsin stain solution. Then, the slices were reacted with a phosphomolybdic acid differentiation solution, stained with aniline blue counterstain, and rinsed with absolute ethanol. The slices were blow-dried, cleared in xylene, and then sealed with neutral gum before observation with a microscope.

2.13 Statistical Analysis

Data were analyzed by GraphPad Prism 8.0.1 (GraphPad Software Inc., San Diego, CA, USA) and expressed as mean ± standard deviation. Kolmogorov-Smirnov test and exploratory descriptive statistics test were used to analyze whether the data conformed to a normal distribution and homogeneity of variance. One-way analysis of variance (ANOVA) and Tukey's post-hoc test were employed in comparison between groups. Comparisons between groups at different time points were analyzed by two-way ANOVA with Bonferroni as a post hoc test. The difference was statistically significant when $p < 0.05$. All the experiments followed randomization and blind analysis to avoid experimental bias.

3. Results

3.1 EGCG Improved HG-Induced Autophagy Impairment in Keratinocytes

To screen suitable EGCG concentration, keratinocytes were treated with a series of EGCG concentrations (0, 6.25, 12.5, 25, 50, and 100 μM) for 24 h, and the cell viability was measured with the CCK-8 assay. No significant effect on cell viability was observed with EGCG at 0, 6.25, 12.5, 25, and 50 μM. However, However, keratinocyte viability was significantly decreased with 100 μM EGCG. Thus, 50 μM EGCG was selected for subsequent experiments (Fig. 1A). To explore the effect of EGCG on autophagy impairment, keratinocytes were first induced with HG (50 mM glucose) for 24 h, and then treated with EGCG for another 24 h, after which the levels of autophagy-related proteins were analyzed. After HG induction, autophagy was impaired in keratinocytes, showing decreased LC3II/LC3I, Beclin1, and ATG5 levels, and increased p62 level. However, after EGCG treatment, LC3II/LC3I, Beclin1, and ATG5 levels raised whereas p62 level declined in HG-treated keratinocytes, and the extent of these changes was EGCG concentration-dependent (Fig. 1B). Collectively, the above results demonstrated that EGCG improved HG-induced autophagy impairment in keratinocytes.

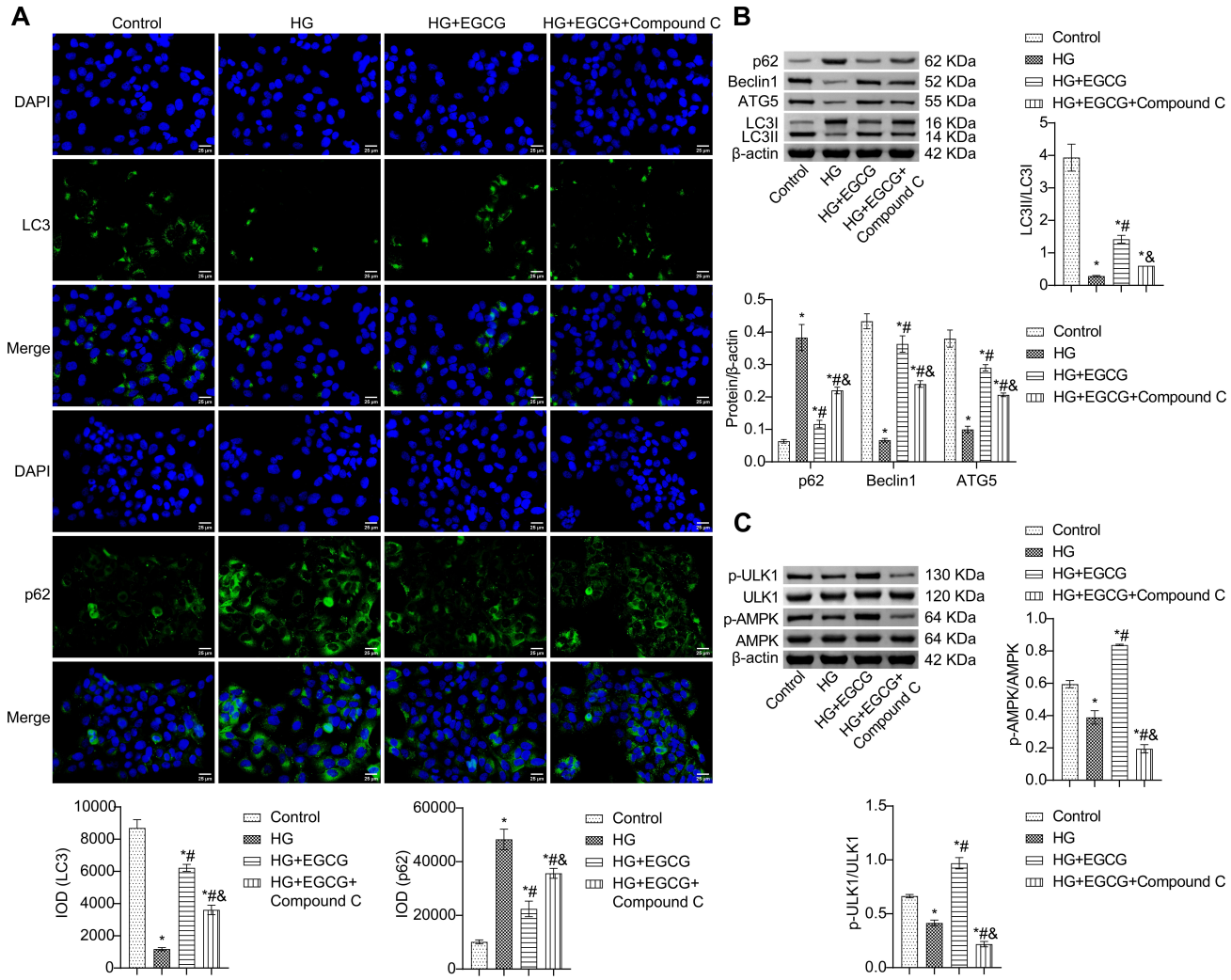

Fig. 2. Activation of the AMPK/ULK1 pathway could promote autophagy induction of EGCG to HG-treated keratinocytes. (A) The levels of LC3 and p62 in keratinocytes were detected by IF staining. (B,C) The levels of p62, Beclin1, ATG5, LC3I, LC3II, p-ULK1, ULK1, p-AMPK, and AMPK in keratinocytes were determined by Western blot. *$p < 0.05$ *vs.* Control, #$p < 0.05$ *vs.* HG, &$p < 0.05$ *vs.* HG + EGCG.

3.2 EGCG Increased Autophagy in HG-Treated Keratinocytes by Activating the AMPK/ULK1 Pathway

To clarify the regulation of the AMPK/ULK1 pathway in autophagy induction by EGCG in HG-treated keratinocytes, an AMPK inhibitor (Compound C) was utilized to intervene, and proteins related to autophagy and the pathway were analyzed. HG induction led to a reduction in LC3, Beclin1, and ATG5 levels while a rise in p62 level in keratinocytes. Compared with the HG group, LC3, Beclin1, and ATG5 levels were raised and p62 level was declined in keratinocytes in the HG + EGCG group. However, the use of Compound C significantly reversed the autophagy induction of EGCG (Fig. 2A,B). Further analysis demonstrated that HG induction decreased the phosphorylation of AMPK and ULK1 in keratinocytes. Compared with the HG group, phosphorylation of AMPK and ULK1 in keratinocytes increased in the HG + EGCG group. However, the use of Compound C significantly reversed the effect of EGCG on AMPK/ULK1 pathway activation (Fig. 2C). These results suggested that EGCG enhanced autophagy in HG-treated keratinocytes by activating the AMPK/ULK1 pathway.

3.3 EGCG Promoted the Proliferation and Migration of HG-Treated Keratinocytes by Enhancing Autophagy

Based on the above results, we further conducted EdU staining, scratch assay, and Western blot analyses on the proliferation and migration of keratinocytes. The proliferation and migration of keratinocytes were significantly inhibited following HG induction. Compared with the HG group, the proliferation, and migration of keratinocytes were significantly raised in the HG + EGCG group. However, the use of Compound C significantly reversed the promoting effects EGCG on the proliferation and migration of keratinocytes (Fig. 3A,B). Through the detection of chemokine CCL2, we observed a decrease in the synthesis of CCL2 in keratinocytes, as well as a decline in the

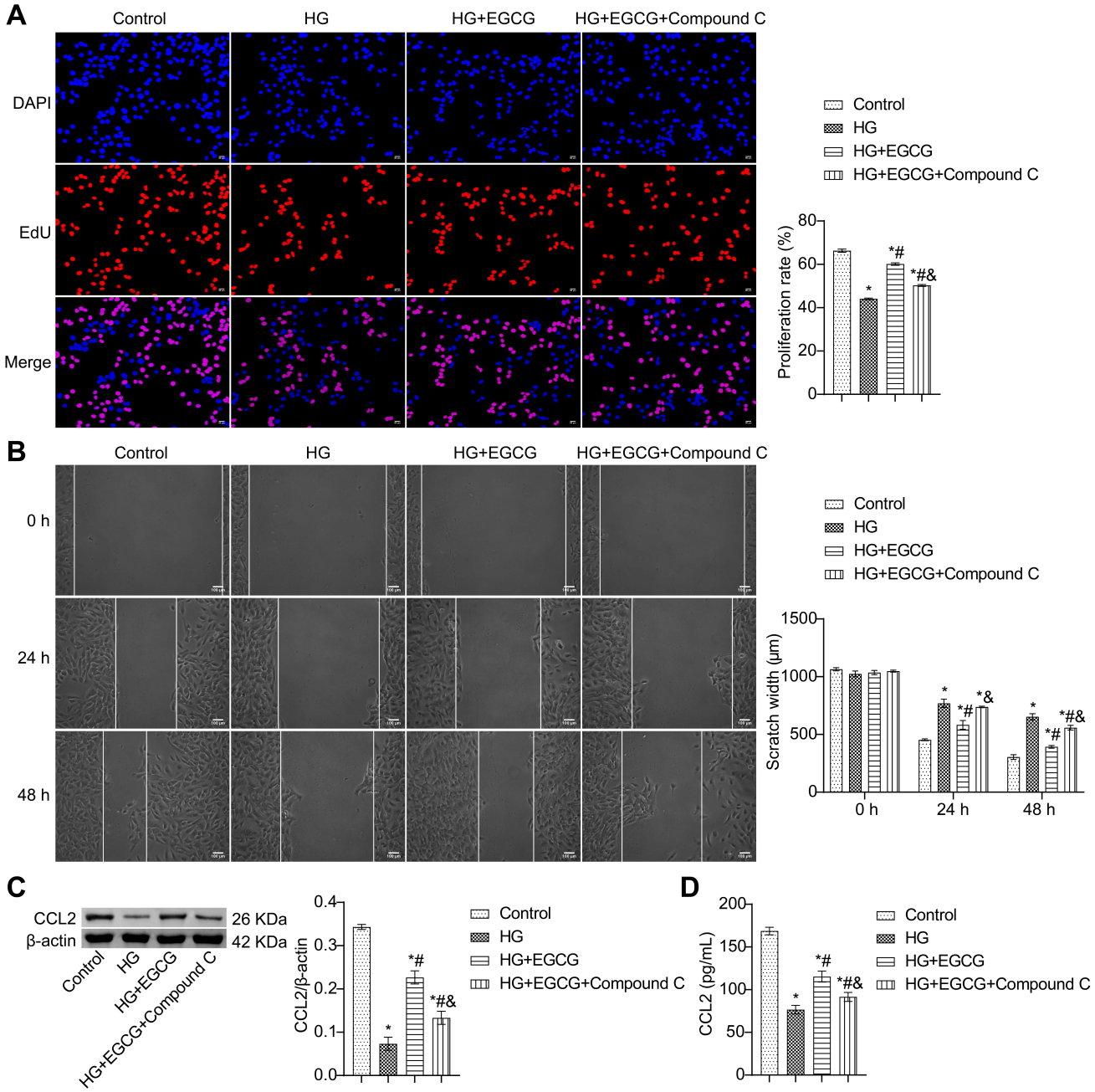

Fig. 3. EGCG promoted the proliferation and migration of HG-treated keratinocytes by enhancing autophagy. (A) EdU staining of keratinocyte proliferation. (B) Scratch assay of keratinocyte migration. (C) The synthesis of CCL2 in keratinocytes was analyzed by Western blot. (D) The content of CCL2 in the keratinocyte culture supernatant was determined by ELISA. *$p < 0.05$ *vs.* Control, #$p < 0.05$ *vs.* HG, &$p < 0.05$ *vs.* HG + EGCG.

content of CCL2 released into the culture supernatant after HG induction. Compared with the HG group, the synthesis and release of CCL2 in keratinocytes were raised in the HG + EGCG group. Notably, the use of Compound C significantly reversed the promoting effects of EGCG on the synthesis and release of CCL2 (Fig. 3C,D). These results displayed that EGCG promoted the proliferation and migration of HG-treated keratinocytes by enhancing autophagy.

3.4 EGCG Promoted Fibroblast Activation by Enhancing Keratinocyte Autophagy

To explore the impact of EGCG-induced keratinocyte autophagy on fibroblasts, the culture supernatant of keratinocytes from different treatment groups was added to the fibroblasts and incubated for 48 h. Fibroblast markers, including α-SMA and Collagen I, were measured by IF staining. The levels of α-SMA and Collagen I in fibroblasts of the HG group were lower than those in the Control group. The levels of α-SMA and Collagen I in fibroblasts of

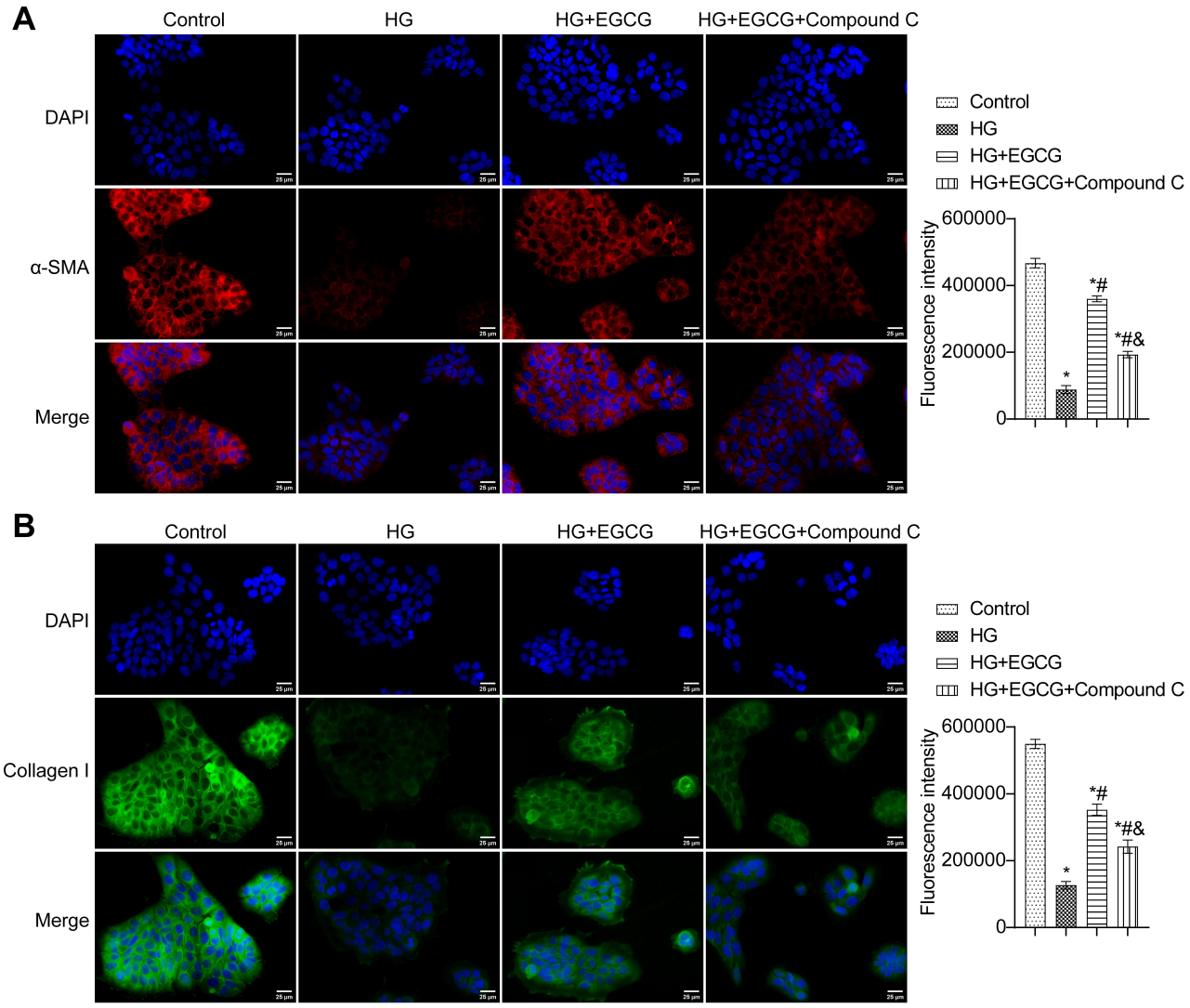

Fig. 4. Autophagy induction of EGCG on keratinocytes promoted fibroblast activation. (A,B) The levels of α-SMA and Collagen I in fibroblasts were analyzed by IF staining. *$p < 0.05$ *vs.* Control, #$p < 0.05$ *vs.* HG, &$p < 0.05$ *vs.* HG + EGCG.

HG + EGCG group were raised compared with those in the HG group. However, treatment with Compound C significantly reversed the activating effects of EGCG on fibroblasts (Fig. 4A,B). Together, these results showed that EGCG promoted fibroblast activation by enhancing keratinocyte autophagy.

3.5 EGCG Enhanced Epidermal Autophagy through the AMPK/ULK1 Pathway to Promote Diabetic Wound Healing

To explore the effect of EGCG on DCU, wounds on the back of DM rats were intervened with EGCG and Compound C, and the wound healing process was monitored on days 0–14. In the Control group, the wound area was gradually decreased with time and was fully epithelialized by day 14. By contrast, the wound in the DM group healed slowly and was not completely healed by day 14. However, wound healing in the DM + EGCG group was significantly improved, with the wound appearing nearly fully healed by day 14. Notably, the use of Compound C significantly reversed the beneficial effect of EGCG on wound healing (Fig. 5A,B). HE staining of the wounds on day 14 showed that the granulation tissue was reduced, and the re-epithelialization was weakened, accompanied by many inflammatory infiltrates in the DM group compared with the Control group. After EGCG intervention, inflammatory infiltration decreased, granulation tissue increased, and re-epithelialization enhanced. Unfortunately, the treatment with Compound C significantly reversed the pro-epithelialization effect of EGCG (Fig. 5C). Further analysis showed that compared with the Control group, the levels of LC3II/LC3I, Beclin1, ATG5, and the phosphorylation of AMPK and ULK1 declined in the DM group, whereas the level of p62 was increased. After EGCG intervention, the levels of LC3II/LC3I, Beclin1, ATG5, and phosphorylation of AMPK and ULK1 were increased, whereas the level of p62 was decreased. Again, the use of Compound C significantly reversed the promoting effects of EGCG on

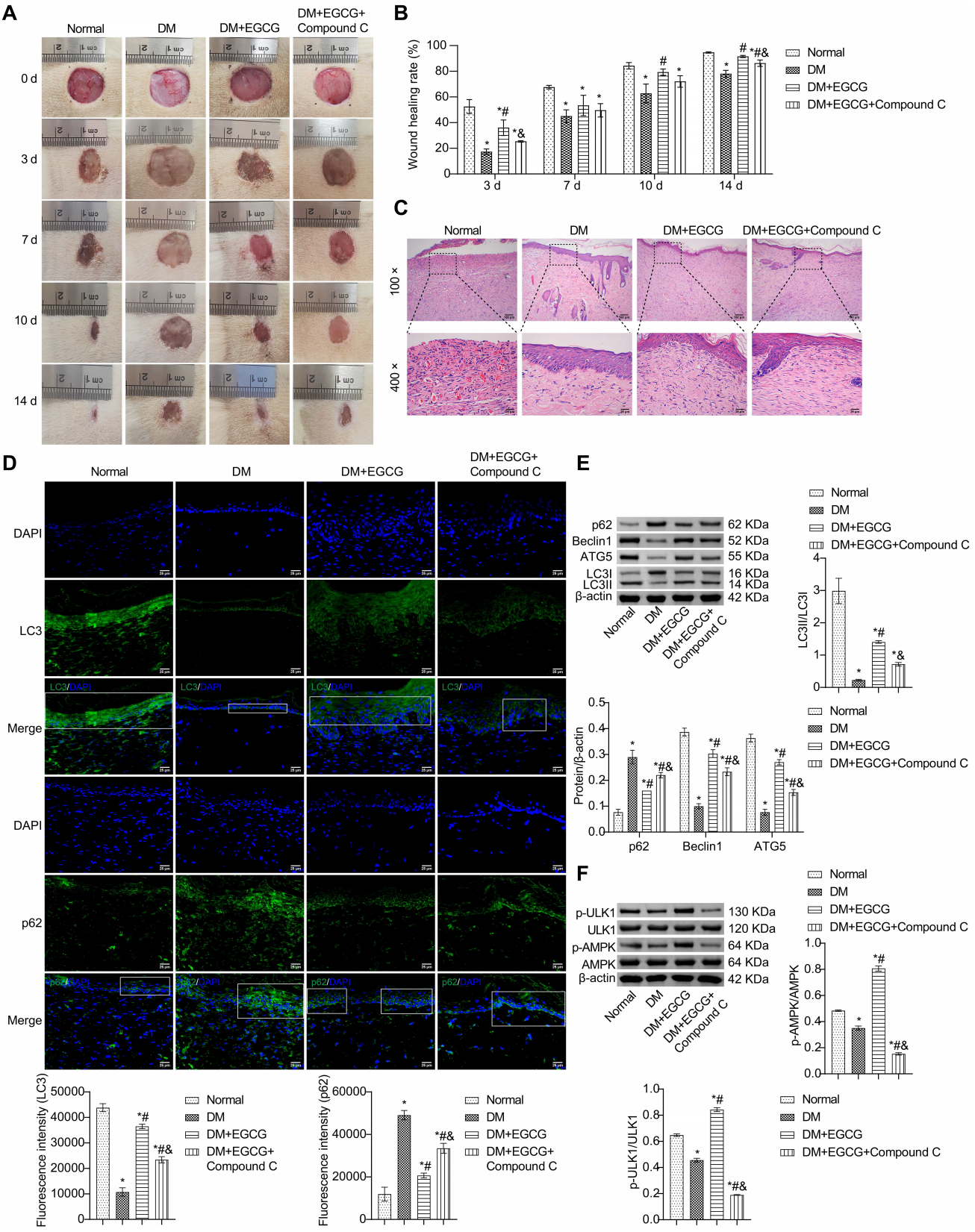

Fig. 5. EGCG enhanced epidermal autophagy through the AMPK/ULK1 pathway to promote diabetic wound healing. (A) Wound images. (B) Wound healing rate. (C) Wound epithelialization was observed on day 14 by HE staining. (D) The levels of LC3 and p62 in wounds on day 14 were analyzed by IF staining. (E,F) The levels of p62, Beclin1, ATG5, LC3I, LC3II, p-ULK1, ULK1, p-AMPK, and AMPK in wounds on day 14 were analyzed by Western blot. *$p < 0.05$ *vs.* Control, #$p < 0.05$ *vs.* HG, &$p < 0.05$ *vs.* HG + EGCG.

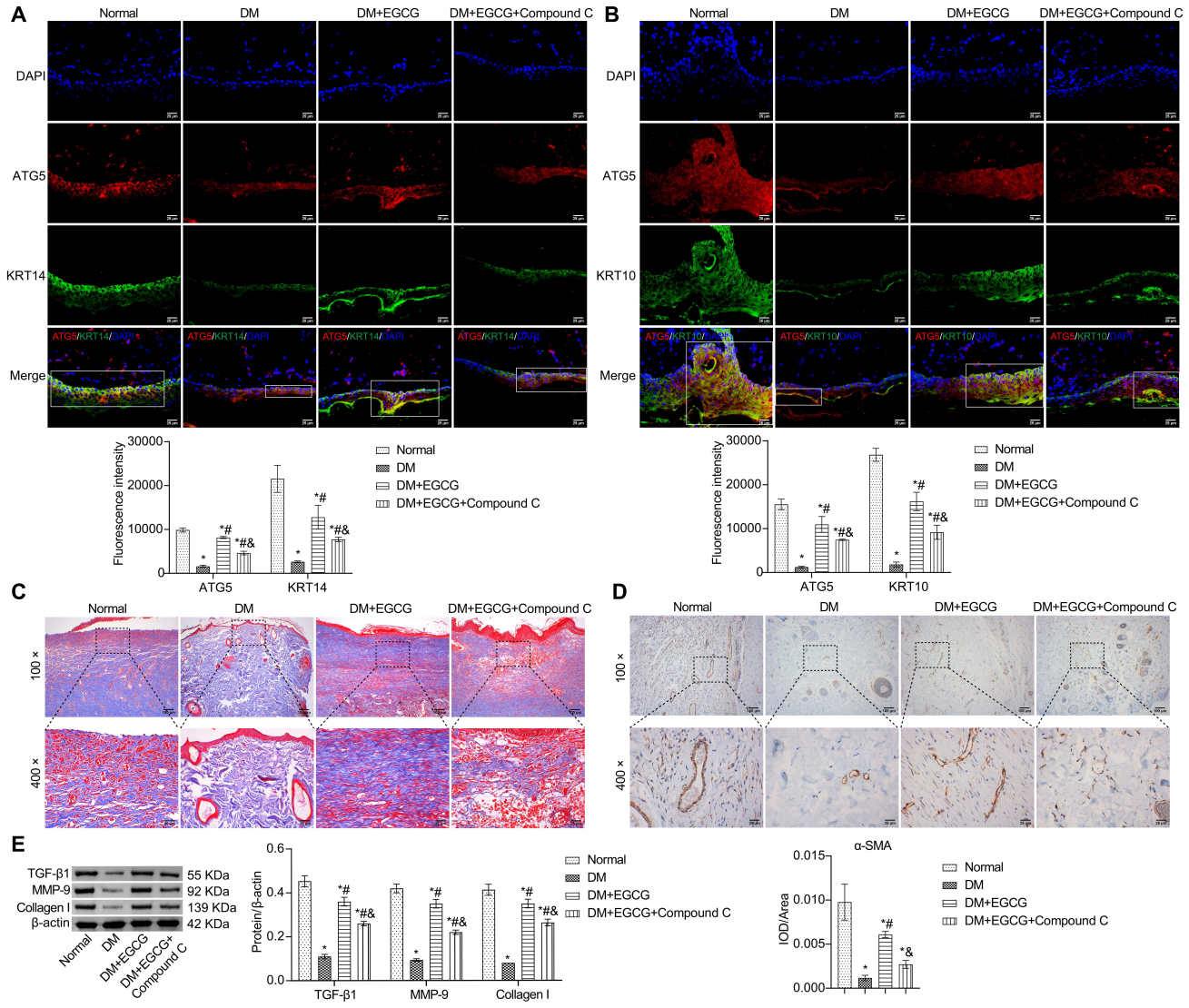

Fig. 6. EGCG promoted keratinocyte proliferation and differentiation and fibroblast activation by enhancing epidermal autophagy. (A,B) The levels of ATG5, KRT10, and KRT14 in wounds on day 14 were analyzed by IF staining. (C) Collagen deposition in wounds on day 14 was assessed by Masson staining. (D) The level of α-SMA in wounds on day 14 was assayed by IHC staining. (E) The levels of TGF-β1, Collagen I, and MMP-9 in wounds on day 14 were analyzed by Western blot. *$p < 0.05$ *vs.* Control, #$p < 0.05$ *vs.* HG, &$p < 0.05$ *vs.* HG + EGCG. IHC, immunohistochemistry.

epidermal autophagy and AMPK/ULK1 pathway activation (Fig. 5D–F). These results illustrated that EGCG enhanced epidermal autophagy through the AMPK/ULK1 pathway to promote diabetic wound healing.

3.6 EGCG Promoted Keratinocyte Proliferation and Differentiation and Fibroblast Activation by Enhancing Epidermal Autophagy

We examined keratinocyte proliferation and differentiation and fibroblast activation-related proteins in the wound on day 14. IF staining showed a decrease in the number of ATG5/KRT14- and ATG5/KRT10-positive cells in the DM group compared with the Normal group. After EGCG intervention, the number of ATG5/KRT14- and ATG5/KRT10-positive cells was increased. However, the use of Compound C significantly reversed the effects of EGCG (Fig. 6A,B). Masson staining displayed that collagen deposition was reduced and collagen fibers were disordered in the DM group compared with the Normal group. After EGCG intervention, collagen deposition recovered and the arrangement of collagen fibers tended to be orderly. However, the use of Compound C significantly reversed the promotion of EGCG on collagen deposition (Fig. 6C). Further study displayed that the levels of α-SMA, TGF-β1, Collagen I, and MMP-9 were downregulated in the DM group compared with the Normal group. The levels of α-SMA, TGF-β1, Collagen I, and MMP-9 were upregulated after EGCG intervention. However, the use of Compound C significantly reversed the upregulation of these proteins by EGCG (Fig. 6D,E). These results suggested that EGCG

promoted keratinocyte proliferation and differentiation and fibroblast activation by enhancing epidermal autophagy.

4. Discussion

DM is a common public health problem in modern society. Treatment for DCU, a major complication of DM, is still under investigation. EGCG, as a component of green tea, possesses various properties [37–39]. In addition, EGCG has beneficial effects on skin wound healing [10]. However, the precise mechanism by which EGCG promotes wound healing in DCU remains unknown. Here, our findings suggested that EGCG could promote DCU wound healing by restoring keratinocyte autophagy through the AMPK/ULK1 pathway.

Autophagy, one of the modes of cell death, is believed to exert a key regulatory role in the recovery from diseases [40]. Recently, the role of autophagy in wound healing has attracted attention [41]. Physiological dysfunction of epidermal keratinocytes plays an important role in delayed diabetic wound healing, including impaired autophagy, proliferation, and migration [42]. Damage to keratinocytes and other skin cells from an HG environment is a major cause of poor diabetic wound healing [43]. Here, keratinocyte autophagy was significantly reduced after HG induction. Unsurprisingly, the addition of EGCG upregulated LC3II/LC3I, Beclinl, and ATG5 levels and downregulated p62 level in HG-induced keratinocytes. In related studies, the increased expression of Beclinl, an autophagy-related gene, contributed to burn wound healing [44]. Beclin1/LC3-mediated autophagy may be beneficial to maintain the survival of injured cells [45]. In addition, increasing ATG5/ATG7 levels can promote the functional recovery of keratinocytes under oxidative stress [46]. A previous study showed that p62 knockdown enhances keratinocyte motor function [47]. Cell proliferation and migration are important processes in normal wound healing. The recovery of keratinocyte proliferation and migration further verified the ameliorative effect of EGCG on HG injury. CCL2 has the function of promoting angiogenesis and immunomodulatory, and is an important chemokine to accelerate wound healing [48]. The addition of EGCG significantly promoted the synthesis and release of CCL2 in HG-induced keratinocytes. These results suggested that EGCG might promote diabetic wound healing by improving the autophagy injury of keratinocytes and thereby promoting their proliferation and migration.

Among the various types of skin cells, keratinocytes and fibroblasts are the main cells involved in the process of wound healing [49]. Fibroblasts are immune regulatory factors in wound healing that play a major role in the construction and remodeling of extracellular matrix in DCU treatment [50]. MMP-9 is thought to be involved in keratinocyte migration, granulation tissue remodeling, and epithelialization during wound healing [51]. Mice deficient in MMP-9 exhibited disturbed collagen fibrogenesis and delayed epithelialization [52]. Collagen synthesis and deposition are key factors in wound closure and are related to the expression of TGF-β1. TGF-β1 is a wound healing factor that helps activate injured fibroblasts [53]. Diabetic wound healing can be enhanced by increasing the proportion of Collagen I in rats [54]. In addition, the up-regulated expressions of fibrosis genes, TGF-β1 and α-SMA, promoted the wound healing of skin burns [55]. In *in vitro* experiments, fibroblasts were cultured with the supernatant of EGCG-treated keratinocytes. The results showed that α-SMA and Collagen I levels were increased in fibroblasts, indicating that EGCG indirectly promoted the activation of fibroblasts through keratinocytes. In *in vivo* experiments, MMP-9, TGF-β1, Collagen I, and α-SMA levels in neonatal epithelial tissues were up-regulated on day 14 after treatment with EGCG, resulting in an increase in granulation tissue and an accelerated rate of wound healing. These results proved that EGCG promoted the proliferation and differentiation of fibroblasts by inducing collagen production and deposition, thus accelerating the wound healing process of DCU.

Autophagy initiation is mediated by the ULK1 complex, which is regulated by AMPK [56]. In addition, the downregulation of ULK1 has been associated with autophagy injury in DM and its complications [57]. The AMPK signaling pathway plays a major role in autophagy induction, and the upregulation of p-AMPK expression can induce glucose metabolism [58]. The use of EGCG significantly promoted the phosphorylation of AMPK and ULK1 in HG-induced keratinocytes and neonatal epithelial tissues in DM rats. Therefore, we speculated that the role of EGCG is related to the AMPK/ULK1 pathway. To further verify the regulatory role of the AMPK/ULK1 pathway in EGCG promoting diabetic wound healing, Compound C, a selective AMPK inhibitor, was selected for intervention *in vitro* and *in vivo*. As a result, autophagy, proliferation, and migration of keratinocytes and activation of fibroblasts were inhibited, and collagen synthesis and deposition were reduced, thus delaying epithelialization and wound healing. These results displayed that EGCG accelerated diabetic wound healing through activation of the AMPK/ULK1 pathway.

Despite the promising findings of this study, there are several limitations that need to be addressed in future research. Firstly, all experiments were performed using *in vitro* and *in vivo* models, and the findings may not necessarily reflect the complexities of diabetic wound healing in humans. Further clinical trials are needed to validate the therapeutic potential of EGCG in diabetic wound healing. Secondly, while the study focused on the role of EGCG in keratinocyte autophagy, the potential effects on other pathways involved in wound healing, such as oxidative stress and inflammation, were not investigated. Future studies should explore the comprehensive mechanisms underlying the therapeutic effects of EGCG in diabetic wound healing.

Finally, the study only examined the effects of EGCG on the AMPK/ULK1 pathway. Other pathways that regulate autophagy may also be involved in the therapeutic effects of EGCG, and further studies are needed to elucidate these mechanisms.

5. Conclusions

To conclude, EGCG promoted diabetic wound healing, which might be achieved by restoring keratinocyte autophagy through the AMPK/ULK1 pathway to promote the activation of keratinocytes and fibroblasts. This study will provide value for the study of the pathogenesis and treatment of DCU.

Abbreviations

DCU, Diabetic cutaneous ulcers; DM, diabetes mellitus; EGCG, Epigallocatechin gallate; TNF-α, tumor necrosis factor-α; HG, High glucose; CCL2, C-C motif chemokine ligand 2; AMPK, AMP-activated protein kinase; ULK1, Unc-51 like kinase-1; STZ, streptozotocin; DMEM, Dulbecco's modified Eagle's medium; FBS, fetal bovine serum; IF, Immunofluorescence; EdU, 5-Ethynyl-2′-deoxyuridine; CCK-8, Cell counting kit-8; OD, optical density; NC, nitrocellulose; BSA, bovine serum albumin; α-SMA, alpha-smooth muscle actin; KRT10, keratin 10; ELISA, Enzyme-linked immunosorbent assay; HE, Hematoxylin-eosin; IHC, Immunohistochemistry; VEGF, vascular endothelial growth factor; IL-8, interleukin-8; LC3, microtubule-associated protein 1 light chain 3; ATG5, autophagy-related protein 5; PBS, phosphate-buffered saline; SDS-PAGE, sodium dodecyl sulfate-polyacrylamide gel electrophoresis; HRP, horseradish peroxidase; DAPI, 4′,6-diamidino-2-phenylindole; DAB, diaminobenzidine; p-, phosphorylated-.

Availability of Data and Materials

All raw data can be provided upon request.

Author Contributions

LJ and ML designed the research study. CT, YF, TC, ZZ, and XH performed the research. CT and YF analyzed the data. CT and YF wrote the manuscript. All authors contributed to editorial changes in the manuscript. All authors read and approved the final manuscript. All authors have participated sufficiently in the work and agreed to be accountable for all aspects of the work.

Ethics Approval and Consent to Participate

This research has been approved by the Institutional Animal Ethics Committee of South China University (No. LSZ2023D110H).

Acknowledgment

Not applicable.

Funding

This research was supported by Natural Science Foundation of Changsha (No. kq2208441 and kq2208446), Key Project in Changsha Central Hospital (No. YNKY202107), and Hunan Clinical Medical Technology Innovation Guidance Project (No. 2020SK53304).

Conflict of Interest

The authors declare no conflict of interest.

References

[1] Nie X, Zhang H, Shi X, Zhao J, Chen Y, Wu F, *et al*. Asiaticoside nitric oxide gel accelerates diabetic cutaneous ulcers healing by activating Wnt/β-catenin signaling pathway. International Immunopharmacology. 2020; 79: 106109.

[2] Nie X, Zhao J, Ling H, Deng Y, Li X, He Y. Exploring microRNAs in diabetic chronic cutaneous ulcers: Regulatory mechanisms and therapeutic potential. British Journal of Pharmacology. 2020; 177: 4077–4095.

[3] Ivanov E, Akhmetshina M, Erdiakov A, Gavrilova S. Sympathetic System in Wound Healing: Multistage Control in Normal and Diabetic Skin. International Journal of Molecular Sciences. 2023; 24: 2045.

[4] Paschou SA, Stamou M, Vuagnat H, Tentolouris N, Jude E. Pain management of chronic wounds: Diabetic ulcers and beyond. Maturitas. 2018; 117: 17–21.

[5] Wang D, Gao Q, Wang T, Kan Z, Li X, Hu L, *et al*. Green tea polyphenols and epigallocatechin-3-gallate protect against perfluorodecanoic acid induced liver damage and inflammation in mice by inhibiting NLRP3 inflammasome activation. Food Research International. 2020; 127: 108628.

[6] Ungarala R, Munikumar M, Sinha SN, Kumar D, Sunder RS, Challa S. Assessment of Antioxidant, Immunomodulatory Activity of Oxidised Epigallocatechin-3-Gallate (Green Tea Polyphenol) and Its Action on the Main Protease of SARS-CoV-2-An In Vitro and In Silico Approach. Antioxidants. 2022; 11: 294.

[7] Yang R, Chen J, Jia Q, Yang X, Mehmood S. Epigallocatechin-3-gallate ameliorates renal endoplasmic reticulum stress-mediated inflammation in type 2 diabetic rats. Experimental Biology and Medicine. 2022; 247: 1410–1419.

[8] Gordon NC, Wareham DW. Antimicrobial activity of the green tea polyphenol (-)-epigallocatechin-3-gallate (EGCG) against clinical isolates of Stenotrophomonas maltophilia. International Journal of Antimicrobial Agents. 2010; 36: 129–131.

[9] Farhan M. Green Tea Catechins: Nature's Way of Preventing and Treating Cancer. International Journal of Molecular Sciences. 2022; 23: 10713.

[10] Xu FW, Lv YL, Zhong YF, Xue YN, Wang Y, Zhang LY, *et al*. Beneficial Effects of Green Tea EGCG on Skin Wound Healing: A Comprehensive Review. Molecules. 2021; 26: 6123.

[11] Trompezinski S, Denis A, Schmitt D, Viac J. Comparative effects of polyphenols from green tea (EGCG) and soybean (genistein) on VEGF and IL-8 release from normal human keratinocytes stimulated with the proinflammatory cytokine TNFalpha. Archives of Dermatological Research. 2003; 295: 112–116.

[12] Ud-Din S, Foden P, Mazhari M, Al-Habba S, Baguneid M, Bulfone-Paus S, *et al*. A Double-Blind, Randomized Trial Shows the Role of Zonal Priming and Direct Topical Application of Epigallocatechin-3-Gallate in the Modulation of Cutaneous Scarring in Human Skin. Journal of Investigative Dermatology. 2019; 139: 1680–1690.e16.

[13] Huang Y, Zhu Q, Yang X, Xu H, Sun B, Wang X, *et al*. Wound

healing can be improved by (-)-epigallocatechin gallate through targeting Notch in streptozotocin-induced diabetic mice. The FASEB Journal. 2019; 33: 953–964.
[14] Mitchell K, Szekeres C, Milano V, Svenson KB, Nilsen-Hamilton M, Kreidberg JA, *et al*. Alpha3beta1 integrin in epidermis promotes wound angiogenesis and keratinocyte-to-endothelial-cell crosstalk through the induction of MRP3. Journal of Cell Science. 2009; 122: 1778–1787.
[15] Rognoni E, Watt FM. Skin Cell Heterogeneity in Development, Wound Healing, and Cancer. Trends in Cell Biology. 2018; 28: 709–722.
[16] den Dekker A, Davis FM, Kunkel SL, Gallagher KA. Targeting epigenetic mechanisms in diabetic wound healing. Translational Research. 2019; 204: 39–50.
[17] Yu T, Zuber J, Li J. Targeting autophagy in skin diseases. Journal of Molecular Medicine. 2015; 93: 31–38.
[18] Li L, Zhang J, Zhang Q, Zhang D, Xiang F, Jia J, *et al*. High Glucose Suppresses Keratinocyte Migration Through the Inhibition of p38 MAPK/Autophagy Pathway. Frontiers in Physiology. 2019; 10: 24.
[19] Darby I, Laverdet B, Bonté F, Desmoulière A. Fibroblasts and myofibroblasts in wound healing. Clinical, Cosmetic and Investigational Dermatology. 2014; 7: 301–311.
[20] Werner S, Krieg T, Smola H. Keratinocyte–Fibroblast Interactions in Wound Healing. Journal of Investigative Dermatology. 2007; 127: 998–1008.
[21] Qiang L, Yang S, Cui Y, He Y. Keratinocyte autophagy enables the activation of keratinocytes and fibroblastsand facilitates wound healing. Autophagy. 2021; 17: 2128–2143.
[22] Jeon SM. Regulation and function of AMPK in physiology and diseases. Experimental and Molecular Medicine. 2016; 48: e245.
[23] Joshi T, Singh AK, Haratipour P, Sah AN, Pandey AK, Naseri R, *et al*. Targeting AMPK signaling pathway by natural products for treatment of diabetes mellitus and its complications. Journal of Cellular Physiology. 2019; 234: 17212–17231.
[24] Madhavi YV, Gaikwad N, Yerra VG, Kalvala AK, Nanduri S, Kumar A. Targeting AMPK in Diabetes and Diabetic Complications: Energy Homeostasis, Autophagy and Mitochondrial Health. Current Medicinal Chemistry. 2019; 26: 5207–5229.
[25] Yao Z, Xu L, Jin L, Wang T, Wang B, Li J, *et al*. K-Carrageenan oligosaccharides induce microglia autophagy through AMPK/ULK1 pathway to regulate their immune response. International Journal of Biological Macromolecules. 2022; 194: 198–203.
[26] Wang W, Jiang J, Huang Y, Peng F, Hu T, Wu J, *et al*. Aconitine induces autophagy via activating oxidative DNA damage-mediated AMPK/ULK1 signaling pathway in H9c2 cells. Journal of Ethnopharmacology. 2022; 282: 114631.
[27] Kim J, Kundu M, Viollet B, Guan K. AMPK and mTOR regulate autophagy through direct phosphorylation of Ulk1. Nature Cell Biology. 2011; 13: 132–141.
[28] Song J, Liu J, Cui C, Hu H, Zang N, Yang M, *et al*. Mesenchymal stromal cells ameliorate diabetes-induced muscle atrophy through exosomes by enhancing AMPK/ULK1-mediated autophagy. Journal of Cachexia, Sarcopenia and Muscle. 2023; 14: 915–929.
[29] Lu Q, Ding Y, Liu Y, Wang Z, Wu Y, Niu K, *et al*. Metrnl ameliorates diabetic cardiomyopathy via inactivation of cGAS/STING signaling dependent on LKB1/AMPK/ULK1-mediated autophagy. Journal of Advanced Research. 2022. (online ahead of print)
[30] Holczer M, Besze B, Zámbó V, Csala M, Bánhegyi G, Kapuy O. Epigallocatechin-3-Gallate (EGCG) Promotes Autophagy-Dependent Survival via Influencing the Balance of mTOR-AMPK Pathways upon Endoplasmic Reticulum Stress. Oxidative Medicine and Cellular Longevity. 2018; 2018: 6721530.
[31] Nie X, Zhang H, Shi X, Zhao J, Chen Y, Wu F, *et al*. Asiaticoside nitric oxide gel accelerates diabetic cutaneous ulcers healing by activating Wnt/β-catenin signaling pathway. International Immunopharmacology. 2020; 79: 106109.
[32] Jin H, Zhang Z, Wang C, Tang Q, Wang J, Bai X, *et al*. Melatonin protects endothelial progenitor cells against AGE-induced apoptosis via autophagy flux stimulation and promotes wound healing in diabetic mice. Experimental and Molecular Medicine. 2018; 50: 1–15.
[33] Zhang P, He L, Zhang J, Mei X, Zhang Y, Tian H, *et al*. Preparation of novel berberine nano-colloids for improving wound healing of diabetic rats by acting Sirt1/NF-κB pathway. Colloids and Surfaces B: Biointerfaces. 2020; 187: 110647.
[34] Chen C, Li L, Qin H, Huang Z, Xian J, Cai J, *et al*. Effects of Irbesartan Pretreatment on Pancreatic β-Cell Apoptosis in STZ-Induced Acute Prediabetic Mice. Oxidative Medicine and Cellular Longevity. 2018; 2018: 8616194.
[35] Sun M, Xie Q, Cai X, Liu Z, Wang Y, Dong X, *et al*. Preparation and characterization of epigallocatechin gallate, ascorbic acid, gelatin, chitosan nanoparticles and their beneficial effect on wound healing of diabetic mice. International Journal of Biological Macromolecules. 2020; 148: 777–784.
[36] Cao M, Fang J, Wang X, Wang Y, Duan K, Ye F, *et al*. Activation of AMP-activated protein kinase (AMPK) aggravated postoperative cognitive dysfunction and pathogenesis in aged rats. Brain Research. 2018; 1684: 21–29.
[37] Gan R, Li H, Sui Z, Corke H. Absorption, metabolism, anticancer effect and molecular targets of epigallocatechin gallate (EGCG): an updated review. Critical Reviews in Food Science and Nutrition. 2018; 58: 924–941.
[38] Rasheed NO, Ahmed LA, Abdallah DM, El-Sayeh BM. Nephrotoxic effects of intraperitoneally injected EGCG in diabetic mice: involvement of oxidative stress, inflammation and apoptosis. Scientific Reports. 2017; 7: 40617.
[39] Jhang J, Lu C, Yen G. Epigallocatechin gallate inhibits urate crystals-induced peritoneal inflammation in C57BL/6 mice. Molecular Nutrition and Food Research. 2016; 60: 2297–2303.
[40] Martinet W, Agostinis P, Vanhoecke B, Dewaele M, de Meyer GR. Autophagy in disease: a double-edged sword with therapeutic potential. Clinical Science. 2009; 116: 697–712.
[41] Ren H, Zhao F, Zhang Q, Huang X, Wang Z. Autophagy and skin wound healing. Burns and Trauma. 2022; 10: tkac003.
[42] Hu SC, Lan CE. High-glucose environment disturbs the physiologic functions of keratinocytes: Focusing on diabetic wound healing. Journal of Dermatological Science. 2016; 84: 121–127.
[43] Pan L, Zhang X, Gao Q. Histatin-1 alleviates high-glucose injury to skin keratinocytes through MAPK signaling pathway. Journal of Cosmetic Dermatology. 2022; 21: 6281–6291.
[44] Xiao M, Li L, Hu Q, Ma L, Liu L, Chu W, *et al*. Rapamycin reduces burn wound progression by enhancing autophagy in deep second-degree burn in rats. Wound Repair and Regeneration. 2013; 21: 852–859.
[45] Dong JL, Dong HC, Yang L, Qiu ZW, Liu J, Li H, *et al*. Up-regulation of BAG3 with apoptotic and autophagic activities in maggot extract-promoted rat skin wound healing. Molecular Medicine Reports. 2018; 17: 3807–3812.
[46] Jin J, Zhu K, Tang S, Xiang Y, Mao M, Hong X, *et al*. Trehalose promotes functional recovery of keratinocytes under oxidative stress and wound healing via ATG5/ATG7. Burns. 2022; 38: 1014–1022
[47] Zhang YP, Zhang Q, Deng F, Chen B, Zhang JH, Hu J. Effect of P62 on the migration and motility of human epidermal cell line HaCaT in high glucose microenvironment and its mechanism. Zhonghua Shao Shang Za Zhi. 2022; 38: 1014–1022. (In Chinese)
[48] Whelan DS, Caplice NM, Clover AJP. Mesenchymal stromal

cell derived CCL2 is required for accelerated wound healing. Scientific Reports. 2020; 10: 2642.
[49] Shu F, Gao H, Wu W, Yu S, Zhang L, Liu H, *et al*. Amniotic epithelial cells accelerate diabetic wound healing by protecting keratinocytes and fibroblasts from high-glucose-induced senescence. Cell Biology International. 2022; 46: 755–770.
[50] Liu Y, Liu Y, He W, Mu X, Wu X, Deng J, *et al*. Fibroblasts: Immunomodulatory factors in refractory diabetic wound healing. Frontiers in Immunology. 2022; 13: 918223.
[51] Salo T, Mäkelä M, Kylmäniemi M, Autio-Harmainen H, Larjava H. Expression of matrix metalloproteinase-2 and -9 during early human wound healing. Laboratory Investigation. 1994; 70: 176–182.
[52] Kyriakides TR, Wulsin D, Skokos EA, Fleckman P, Pirrone A, Shipley JM, *et al*. Mice that lack matrix metalloproteinase-9 display delayed wound healing associated with delayed reepithelization and disordered collagen fibrillogenesis. Matrix Biology. 2009; 28: 65–73.
[53] Ueshima E, Fujimori M, Kodama H, Felsen D, Chen J, Durack JC, *et al*. Macrophage-secreted TGF-β(1) contributes to fibroblast activation and ureteral stricture after ablation injury. American Journal of Physiology-Renal Physiology. 2019; 317: F52–f64.
[54] Wang T, Gu Q, Zhao J, Mei J, Shao M, Pan Y, *et al*. Calcium alginate enhances wound healing by up-regulating the ratio of collagen types I/III in diabetic rats. The International Journal of Clinical and Experimental Pathology. 2015; 8: 6636–6645.
[55] Elbialy ZI, Assar DH, Abdelnaby A, Asa SA, Abdelhiee EY, Ibrahim SS, *et al*. Healing potential of Spirulina platensis for skin wounds by modulating bFGF, VEGF, TGF-ß1 and α-SMA genes expression targeting angiogenesis and scar tissue formation in the rat model. Biomed Pharmacother. 2021; 137: 111349.
[56] Pan Z, Li S, Guo H, Li Z, Fei X, Chang S, *et al*. Ebastine exerts antitumor activity and induces autophagy by activating AMPK/ULK1 signaling in an IPMK-dependent manner in osteosarcoma. International Journal of Biological Sciences. 2023; 19: 537–551.
[57] Ma Z, Li L, Livingston MJ, Zhang D, Mi Q, Zhang M, *et al*. P53/microRNA-214/ULK1 axis impairs renal tubular autophagy in diabetic kidney disease. Journal of Clinical Investigation. 2020; 130: 5011–5026.
[58] Wang ZH, Bao XG, Hu JJ, Shen SB, Xu GH, Wu YL. Nicotinamide Riboside Enhances Endothelial Precursor Cell Function to Promote Refractory Wound Healing Through Mediating the Sirt1/AMPK Pathway. Frontiers in Pharmacology. 2021; 12: 671563.